*Progress In Electromagnetics Research C, Vol. 81, 53–62, 2018*

# A Planar Extended Monopulse DOA Estimation Antenna Integrating an RF Multiplier

**Rimi Rashid*, Eisuke Nishiyama, and Ichihiko Toyoda**

**Abstract**—This paper proposes a novel planar direction-of-arrival (DOA) estimation antenna. The estimation capability of phase monopulse DOA estimation antennas is enhanced by integrating an RF multiplier that detects the phase relation between the sum and difference of the two received signals. The proposed antenna provides a wide range of estimation whereas the conventional monopulse DOA estimation antennas determine the angles of half space. A prototype antenna has been fabricated, and the proposed concept was successfully confirmed.

## 1. INTRODUCTION

Direction-of-arrival (DOA) estimation has now become an attractive area for many researchers in the antenna and propagation field. It has a wide range of applications in the field of radar, sonar, electronic surveillance, mobile communications, navigation, etc. In radar applications, DOA techniques are mainly used for air traffic control and target acquisition [1]. Among the other radar tracking techniques, i.e., sequential lobing and conical scan techniques, monopulse radar antennas have gained attention for its high speed, high accuracy and target estimation by a single pulse [2].

Many research activities were presented on monopulse antennas to enrich the research field in this topic. A monopulse microstrip antenna array in a single layer was proposed to achieve two dimensional monopulse performance [3]. Four 3-dB hybrid couplers and several 90° delay lines are used as a comparator in this design. A multilayer $4 \times 4$ microstrip patch antenna was introduced to broaden the impedance bandwidth of the antenna in C-band [4]. Another monopulse antenna was designed by integrating an electromagnetically coupled (EMCP) microstrip antenna array structure and used a rat-race hybrid instead of a branch line coupler as a comparator so that it can be used as a transmitter in addition to a receiver [5]. A dual probe fed single aperture monopulse antenna was presented to eliminate complex phasing networks and aperture arrangement of the antenna. This structure consists of a slot embedded patch, two probe inputs and a 180° directional coupler [6]. The DOA estimation concept based on monopulse mechanism has already been discussed, and the classical monopulse concepts are extended to a general complex monopulse concept which can utilize information from side lobes by using phase shift of the signals [7].

We have also proposed planar DOA estimation antennas based on the phase monopulse mechanism [8, 9]. These antennas are based on the conventional phase monopulse mechanism where only the amplitude of the sum ($\Sigma$) and difference ($\Delta$) of the two received signals are evaluated. Therefore, these antennas detect the arrival angle in only the half plane of the space. In order to achieve wide range of estimation angles, we have also proposed an RF multiplier integrated planar antenna which determines the phase relation between $\Sigma$ and $\Delta$ signals [10]. As only the phase relation between $\Sigma$ and $\Delta$ signals is detected and their amplitudes are not obtained in this design, the DOA operation cannot be performed by this structure.

*Received 9 November 2017, Accepted 23 January 2018, Scheduled 4 February 2018*
* Corresponding author: Rimi Rashid (rimirashid24@ceng.ec.saga-u.ac.jp).
The authors are with the Graduate School of Science and Engineering, Saga University, 1 Honjo-machi, Saga-shi, Saga 840-8502, Japan.

In this paper, a novel 10-GHz DOA estimation antenna integrating an RF multiplier is proposed to enhance the estimation capability of arrival angles. This antenna consists of microstrip lines and slot lines on both sides of the substrate and microwave circuits such as a magic-T and RF multiplier are integrated with the antenna elements. The proposed antenna has a wide range of the DOA estimation capability by effectively using the phase relation of the $\Sigma$ and $\Delta$ signals as well as their amplitudes. A prototype antenna was designed, fabricated and experimentally evaluated. The configuration and basic operation principle of the proposed DOA estimation antenna are discussed in Section 2. In Section 3, the structure and design of the antenna which integrates microstrip antennas, magic-Ts, an RF multiplier and power dividers are described. Section 4 demonstrates a prototype DOA estimation antenna designed at the 10-GHz frequency band. The measured results of the radiation pattern of the $\Sigma$ and $\Delta$ signals and DOA estimation performance are highlighted in this section. Finally, Section 5 concludes the paper.

## 2. DIRECTION OF ARRIVAL PRINCIPLE

### 2.1. Configuration

Figure 1 illustrates a basic block diagram of the proposed extended monopulse DOA estimation antenna composed of two antennas, a magic-T, an RF multiplier and two detectors. As magic-T provides in-phase or anti-phase power division according to the input and output ports, the sum ($\Sigma$) and difference ($\Delta$) of the signals received by the two antennas are separately obtained. The amplitudes of the $\Sigma$ and $\Delta$ signals are detected by the detectors. The RF multiplier is used to detect the phase relation between the $\Sigma$ and $\Delta$ signals and it provides sign of the $\Delta$ signal. The direction of the received arrival wave, i.e., plus or minus of the arrival angle $\theta$, depends on this sign of the $\Delta$ signal.

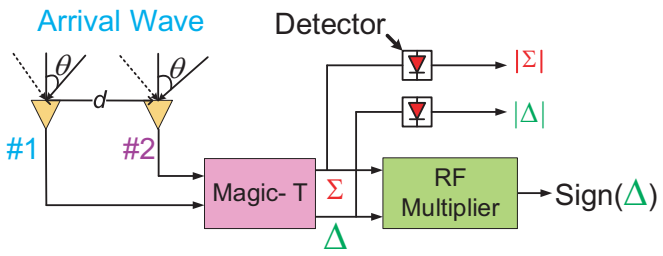


**Figure 1.** Block Diagram of the proposed DOA estimation antenna concept. Sum ($\Sigma$) and difference ($\Delta$) of the two received signals are generated by a magic-T. Sign of $\Delta$ signal can be obtained from the output of an RF multiplier.

### 2.2. Operating Principle

Figure 2 shows the basic operating principle of the proposed extended monopulse DOA estimation antenna with vector diagrams. A radio wave arriving from an angle $\theta$ is received by two antenna elements #1 and #2 with a phase difference $\varphi$. In the vector diagrams, the blue and purple arrows show the signals received by the antenna elements #1 and #2, respectively. The red and green arrows show the $\Sigma$ and $\Delta$ signals, respectively. In the scenario of Figure 2(a), the radio wave comes from the left side of the antennas. In this case, the arrival angle $\theta$ is defined as negative. On the other hand, $\theta$ is defined as positive in the scenario of Figure 2(b).

When two signals received by the two antenna elements #1 and #2 have different phases with the same amplitude, sum ($\Sigma$) and difference ($\Delta$) of the received signals can be expressed by the following equations by assuming the two antenna elements to be isotropic:

$$\Sigma = Ae^{j\frac{\varphi}{2}} + Ae^{-j\frac{\varphi}{2}} = 2A\cos\left(\frac{\varphi}{2}\right) \tag{1}$$

$$\Delta = Ae^{j\frac{\varphi}{2}} - Ae^{-j\frac{\varphi}{2}} = 2jA\sin\left(\frac{\varphi}{2}\right) \tag{2}$$

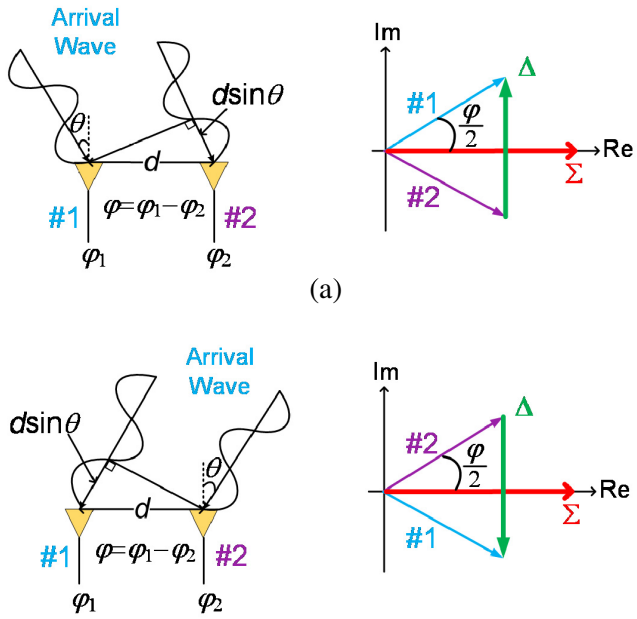


**Figure 2.** Basic operating principle of the proposed DOA estimation antenna. (a) When, $\theta < 0$, $\Delta$ is advanced from $\Sigma$. (b) When $\Delta > 0$, $\Delta$ lags $\Sigma$.

where $A$ and $\varphi$ $(= \varphi_1 - \varphi_2)$ are the amplitude and phase difference between two received signals, respectively.

From the vector diagram shown in Figure 2 and Eqs. (1) and (2), the phase monopulse DOA estimation principle can be explained. The phase difference $\varphi$ is expressed as following equation:

$$\begin{aligned} \tan\frac{\varphi}{2} &= \frac{|\Delta|}{|\Sigma|} \\ \varphi &= 2\tan^{-1}\frac{|\Delta|}{|\Sigma|}. \end{aligned} \tag{3}$$

The phase monopulse mechanism can relate the arrival angle $(\theta)$ and their phase difference $(\varphi)$ of the two received signals by following expression:

$$\theta = \sin^{-1}\left(\frac{\lambda\varphi}{2\pi d}\right) \tag{4}$$

where $d$ is the antenna separation, and $\lambda$ is the wavelength. Thus the monopulse mechanism can be expressed by the following Eq. (5), where the amplitude of the sum $(|\Sigma|)$ and difference $(|\Delta|)$ of the two received signals are used to determine the arrival angle [8–10].

$$\theta = \sin^{-1}\left(\frac{\lambda}{\pi d}\tan^{-1}\frac{|\Delta|}{|\Sigma|}\right). \tag{5}$$

Conventional monopulse DOA estimation antennas determine the arrival angle by only the amplitude of $\Sigma$ and $\Delta$ signals. The phase relation between $\Sigma$ and $\Delta$ signals, i.e., the sign of $\Delta$ signal is not considered. As a result, conventional monopulse DOA estimation antennas cannot determine the sign of arrival angles $\theta$.

The vector diagrams illustrated in Figure 2 indicate two different scenarios. From the vector diagrams and Eqs. (1) and (2), it is clarified that the phase difference between $\Sigma$ and $\Delta$ signals is always 90°. As shown in the vector diagrams, the phase relation between two received signals can be determined by calculating the phase relation between $\Sigma$ and $\Delta$ signals. Figure 2(a) shows #1 leads #2 and $\Delta$ is advanced from $\Sigma$. The arrival angle $\theta$ is negative in this scenario. On the other hand, $\theta$ is

positive and $\Delta$ lags $\Sigma$ in the scenario of Figure 2(b). Thus the antenna can determine the arrival angle on the both sides by evaluating the phase relation between $\Sigma$ and $\Delta$ signals.

An RF multiplier is employed in this structure to determine whether the phase of $\Delta$ signal is advanced or delayed from $\Sigma$ signal. When the $\Sigma$ and $\Delta$ signals are input from two RF inputs of the RF multiplier, the output DC voltage $V_{\mathrm{Mul}}$ can be expressed by following equation:

$$V_{\mathrm{Mul}} \propto |\Sigma| \cdot |\Delta| \cos\left(\varphi_{\Sigma} - \varphi_{\Delta}\right) \tag{6}$$

where $\varphi_{\Sigma}$ and $\varphi_{\Delta}$ are the phases of the two input signals $\Sigma$ and $\Delta$, respectively [14]. As shown in Figure 2 and Eqs. (1) and (2), $\Sigma$ and $\Delta$ signals always have 90° phase difference. Therefore, the feed circuit between the magic-T and RF multiplier has to be designed to give an additional 90° phase difference between the $\Sigma$ and $\Delta$ signals so that $\varphi_{\Sigma} - \varphi_{\Delta}$ has a value of 0° or 180°. When the signal inputs are in phase, i.e., $\varphi_{\Sigma} - \varphi_{\Delta} = 0°$, a positive voltage is obtained as $V_{\mathrm{Mul}}$. On the other hand, if the input signals are in opposite phases, i.e., $\varphi_{\sum} - \varphi_{\Delta} = 180°$, a negative voltage is obtained. This makes it possible to discriminate between in-phase and anti-phase based on the positive and negative of the DC voltage output. Depending on the sign of the output voltage, the direction of the received arrival wave can be determined.

## 3. DOA ANTENNA DESIGN

### 3.1. Antenna Structure

Figure 3 shows the structure of the proposed antenna. The proposed antenna consists of four microstrip antennas, two magic-Ts, two power dividers and an RF multiplier. RF signals received by the antennas are combined, and sum ($\Sigma$) and difference ($\Delta$) of the received signals are obtained from magic-Ts. The amplitude of the $\Sigma$ and $\Delta$ signals can be obtained from Port 1 and Port 2, respectively. Two power dividers are integrated in the proposed antenna structure to divide power to the RF multiplier and output ports of the $\Sigma$ and $\Delta$ signals. Sign of the $\Delta$ signal is obtained at the inner conductor of the slot ring of the RF multiplier. Both side MIC technology has been perfectly applied in this proposed antenna structure [11]. The detectors shown in Figure 1 are not integrated in this structure to measure the RF performance of the antenna. However, it is easy to integrate them in the proposed structure as presented in [9].

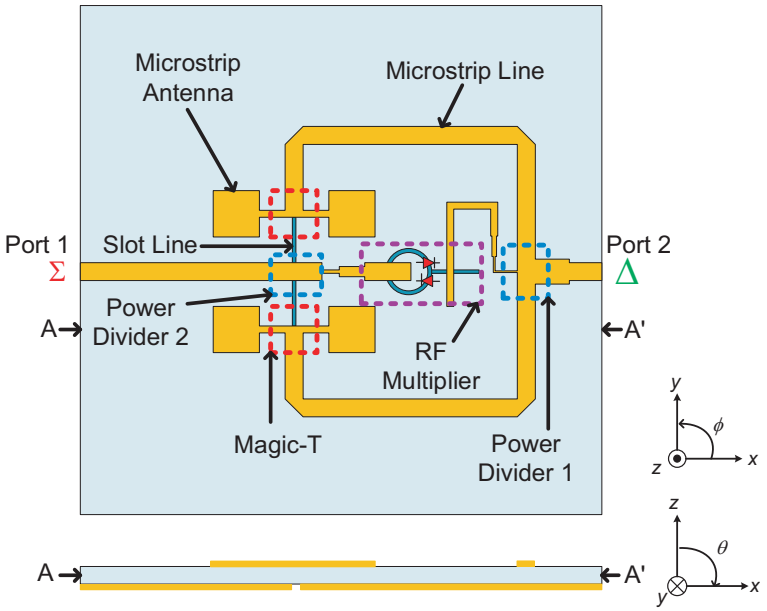


**Figure 3.** Structure of the proposed planar DOA estimation antenna. Two magic-Ts and an RF multiplier employing the both-sided microwave integrated circuit technology are integrated with four antenna elements.

### 3.2. MAGIC-T

Magic-T is a microwave integrated circuit used as a power combiner or divider in all microwave applications [12, 13]. The planar magic-Ts used in the proposed antenna employ a combination of a microstrip line T-junction and slot-to-microstrip line T-branch. Figure 4 illustrates the structure of the magic-T to explain its operation. When two in-phase signals are fed from Port M3 and M4, they are combined and emerge at Port M1 through a microstrip line. On the other hand, two anti-phase signals fed from Port M3 and M4 are combined and emerge at Port M2 through a slot line. Therefore, sum and difference of the two input signals from Port M3 and M4 are separately obtained at Port M1 and M2, respectively. Note that, in Figure 3 the sum ($\Sigma$) and difference ($\Delta$) of the signals received by the two antennas are obtained at Port 1 and 2, respectively, because the feed points of the antennas are located at the opposite side of the antennas.

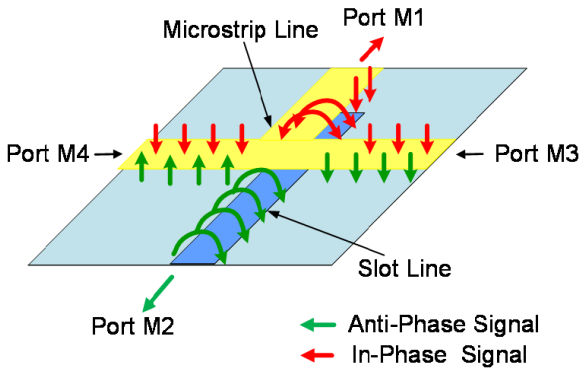


**Figure 4.** Structure of the magic-T integrated in the proposed antenna. It is constructed with a microstrip line T-junction and slot-to-microstrip line T-branch. Sum and difference of the signals are obtained at Port M1 and Port M2, respectively.

### 3.3. RF Multiplier

Figure 5 illustrates the structure of the RF multiplier integrated in the proposed DOA estimation antenna. It consists of two microstrip lines, a slot line, a slot ring and two diodes using both side MIC technology [11].

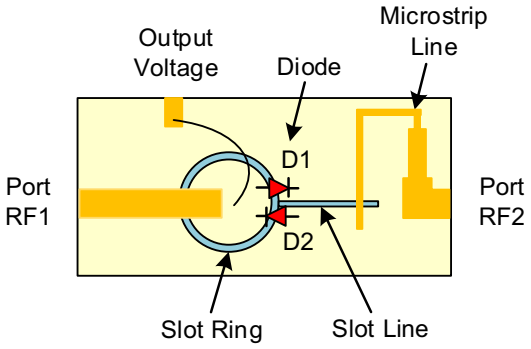


**Figure 5.** Structure of the RF multiplier. Sum ($\Sigma$) and difference ($\Delta$) of the two received signals are fed to Port RF1 and RF2 respectively. By observing the output voltage, sign of $\Delta$ signal can be determined.

$\Sigma$ and $\Delta$ signals fed from Ports RF1 and RF2 propagate to the diodes through the microstrip lines, slot line and slot ring, and they are multiplied by using diodes' nonlinearity. The DC component of the multiplied signal is obtained at the inner conductor of the slot ring. The output DC voltage of the

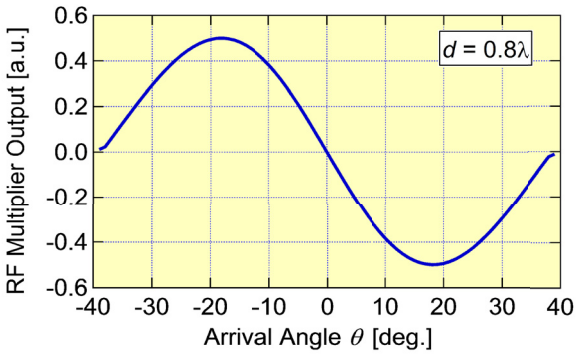


**Figure 6.** Theoretical relation between the RF multiplier output voltage and arrival angle.

RF multiplier $V_{\mathrm{Mul}}$ depends on the phase difference of the input signals from Port RF1 and RF2. $V_{\mathrm{Mul}}$ becomes positive for $\varphi_{\Sigma} - \varphi_{\Delta} = 0°$ and negative for $\varphi_{\sum} - \varphi_{\Delta} = 180°$ according to Eq. (6).

Replacing the amplitude of the sum and difference signals by Eqs. (1) and (2), and the phase difference ($\varphi$) by Eq. (4), the DC voltage of the RF multiplier output and the arrival angle $\theta$ can be related by the following expression:

$$V_{\mathrm{Mul}} \propto |\Sigma| \cdot |\Delta| \cos(\varphi_{\Sigma} - \varphi_{\Delta}) \propto 4A^2 \left| \cos\left\{\frac{\pi d}{\lambda}\sin\theta\right\} \sin\left\{\frac{\pi d}{\lambda}\sin\theta\right\} \right| \cos(\varphi_{\Sigma} - \varphi_{\Delta}). \tag{7}$$

Figure 6 illustrates the relation between the arrival angle $\theta$ and output voltage $V_{\mathrm{Mul}}$ derived from Eq. (7). Here, antennas are assumed isotropic, and $\Delta$ signal has additional 90° phase delay. This additional 90° phase delay is obtained by feed length difference between $\Sigma$ and $\Delta$ signals. The output voltage becomes negative for $\theta > 0$ and positive for $\theta < 0$. In this calculation, antenna element separation is set to 0.8 of the wavelength.

### 3.4. Power Divider

The proposed extended monopulse DOA estimation antenna integrates two power dividers to divide the power of $\Sigma$ and $\Delta$ signals. Powers are distributed from the magic-Ts to the RF multiplier and the output port of the $\Sigma$ and $\Delta$ signals. Power dividers are designed to provide enough power to the output ports and the remaining power to the RF multiplier. Small proportion of power is needed to drive the RF multiplier as the RF multiplier only determines the phase relation of the two input signals.

Figure 7 illustrates two power dividers, power divider 1 and power divider 2. Power divider 1 in Figure 7(a) is a two-way power divider which consists of microstrip lines. Port impedances are designed

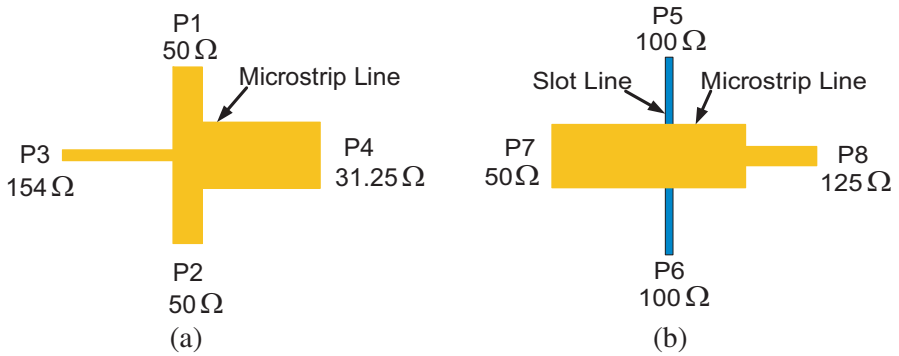


**Figure 7.** Two input two output power dividers used to divide the powers to RF ports and RF multiplier. (a) Power divider 1. This power divider is used to divide the power of $\Delta$ signal. (b) Power divider 2. This power divider is used to divide the power of $\Sigma$ signal.

as 50 Ω, 50 Ω, 154 Ω and 31.25 Ω for P1, P2, P3 and P4, respectively. On the other hand, power divider 2 as shown in Figure 7(b) is formed by microstrip lines and slot lines. 100-Ω port impedance is designed for Port P5 and P6. Port impedances for P7 and P8 are designed as 50 Ω and 125 Ω, respectively. Here, the input signals of Port P1 and P2 are the Δ signals of the magic-T networks. In case of the power divider 2, two Σ signals from magic-Ts are input to Port P5 and P6 and output from Port P7 and P8.

Figure 8 shows the simulated performance of the power dividers. Keysight Technologies' ADS simulation software is used for the simulation. As illustrated in Figure 8(a), reflection coefficient is less than −10 dB for all the input ports P1, P2, P5 and P6. According to Figure 8(b), at power divider 1, around −10 dB of the input power is transferred from P1 and P2 to P3 and around −4.3 dB goes to P4 from P1 and P2. Almost similar characteristics are observed for the power divider 2 where the amount of power transferred from P5 and P6 to P7 and P8 are around −5.5 dB and −9.6 dB, respectively.

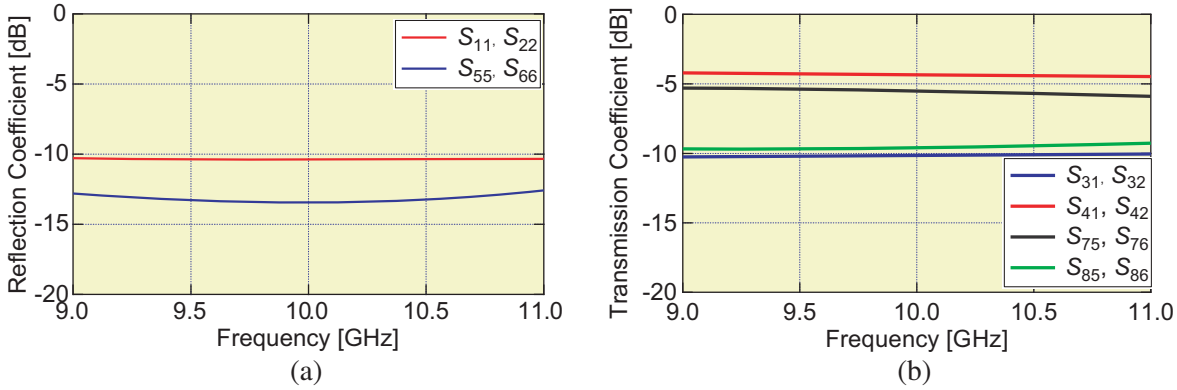


**Figure 8.** Simulated performance of power dividers. (a) Reflection coefficient. (b) Transmission coefficient.

## 4. MEASURED RESULT

### 4.1. Prototype Antenna

Figure 9 shows the top and bottom views of the prototype 10-GHz extended monopulse DOA estimation antenna. In this design, a Teflon fiber ($\varepsilon_r = 2.15$, thickness = 0.8 mm) is used as a substrate material. The size of the proposed antenna is 113 × 113 mm, and the patch size is 9.65 × 9.65 mm. The antenna element separation is 0.8λ (= 24 mm) as the designed center frequency is 10 GHz. Two Schottky diodes (Metelics, MSS30,154-B10B) are used for the RF multiplier. The RF multiplier output can be obtained from the wire connected to the inner conductor of the slot ring as shown in Figure 9(b).

### 4.2. Results and Discussion

The return loss and radiation pattern of the prototype antenna were measured by using a network analyzer (HP8510C) in an anechoic chamber.

Figure 10(a) shows the measured reflection coefficient plots of Port 1 and Port 2 of the designed antenna. Better than 10-dB return loss is observed at 9.85 GHz for both ports. The impedance bandwidth of Δ signal is 1.52% and the impedance bandwidth of 6.94% is obtained for Σ signal. Though the antenna has been designed for 10 GHz, the measured result shows that the minimum reflection coefficient is observed at 9.85 GHz.

Figure 10(b) illustrates the simulated and measured radiation patterns of Σ and Δ signals. Simulation is done by Keysight Technologies' ADS simulation software and diodes are not attached in the simulation process. The simulated gain of this antenna is 12.3 dBi. In the experiment, 9.37 dBi maximum gain is achieved for this antenna. The gain difference between simulation and experiment is 2.97 dB. One of the reasons behind this gain difference is due to diode loss as diode is not considered during simulation. In addition, from our previous experiments in our lab, simulated and experimental

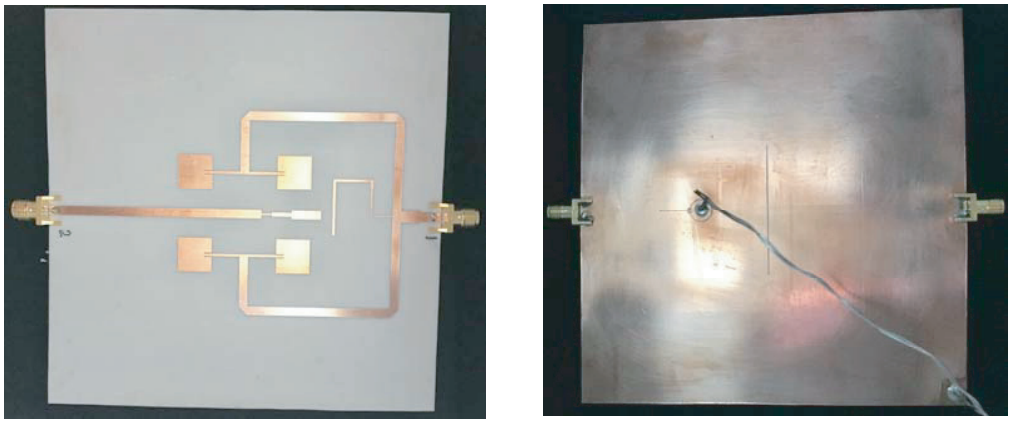

(a) (b)

**Figure 9.** Prototype 10-GHz DOA estimation antenna (Size: $113 \times 113$ mm, $f = 10$ GHz). (a) Top view. (b) Bottom view. The RF multiplier output is acquired from this wire.

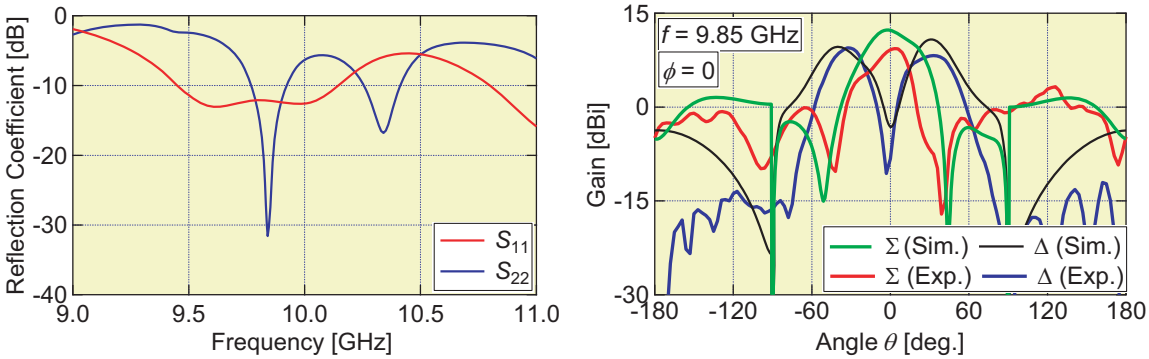


**Figure 10.** Measured reflection coefficient and antenna gain of the proposed DOA estimation antenna integrating an RF multiplier. (a) Reflection coefficient. Less than −10-dB reflection coefficient is obtained at both ports at 9.85 GHz. (b) Radiation pattern.

gain difference of single patch antenna is around 2 dB. Moreover, the influence from welding and fixture when measuring radiation pattern and insertion loss of SMA connectors are also other reasons for the gain difference.

Figure 11 presents the theoretical and measured data of the relation between the arrival angle and $|\Delta|/|\Sigma|$. Theoretical data are calculated from Eq. (5) and measured data are obtained from calculating the measured gain. From this figure, it is obtained that the range of arrival angle is $-38°$ to $38°$ for theory and $-42°$ to $39°$ for measured data.

Figure 12(a) shows the output voltage of the RF multiplier in eight different frequencies. When the arrival angle is greater than zero, the output voltage is negative. When the arrival angle is less than zero, the output voltage is positive. Depending on the sign of this output voltage, sign of the $\Delta$ signal can be determined. In case of 10.2 GHz, the polarity has become opposite. It may be caused due to the phase difference obtained at the input signals of the RF multiplier. All dimensions of the proposed antenna such as the patch size, feed width and feed line difference between $\Sigma$ and $\Delta$ signals are designed at 10 GHz. When frequency changes, the phase of $\Sigma$ and $\Delta$ signals also change because of the different wavelengths for different frequency signals. In other frequencies, there might have possibility that $\Sigma$ and $\Delta$ signals phase become opposite. This phenomena occurs in case of 10.2 GHz.

Figure 12(b) shows the RF multiplier output voltage at four different power densities 0.23, 0.14, 0.09 and 0.06 W/m$^2$. The RF multiplier works even at the power densities as low as 0.06 W/m$^2$.

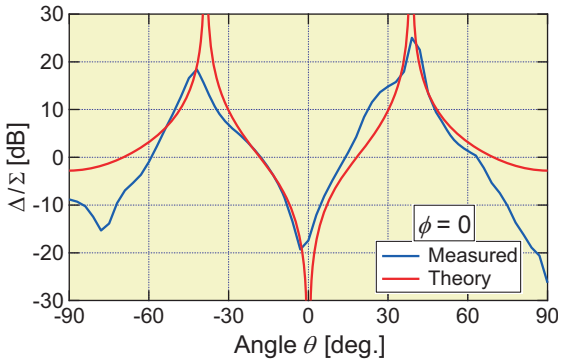


**Figure 11.** Relation between $|\Delta|/|\Sigma|$ and arrival angle $\theta$. Arrival angle can be determined from this plot and sign of the $\Delta$ signal.

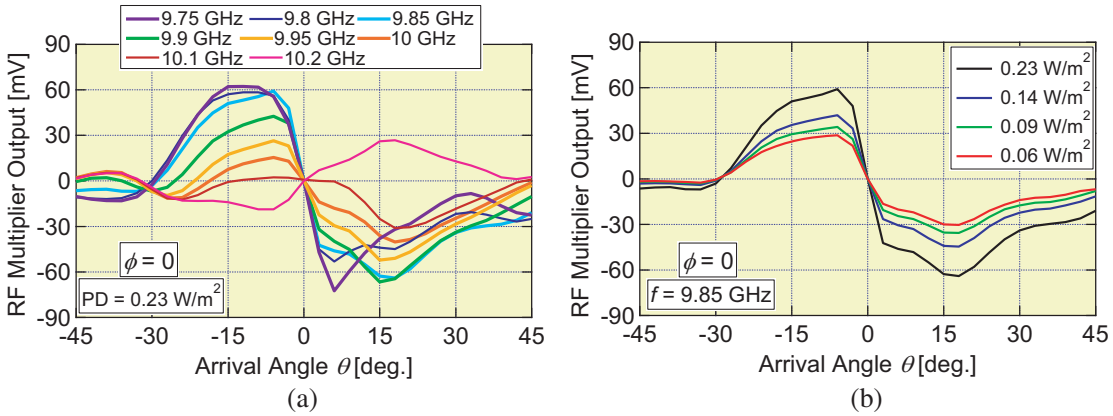


**Figure 12.** Measured RF multiplier output voltage vs. arrival angle. (a) Frequency dependence. (b) Power density dependence.

## 5. CONCLUSION

This paper has presented an RF multiplier integrated planar antenna for extended monopulse DOA estimation. The proposed antenna enhances the estimation range of the arrival angle by evaluating the phase relation between the sum and difference signals, whereas the half angle of the space can be estimated by conventional DOA estimation antennas. The performance of the RF multiplier and radiation characteristics of the antenna have been experimentally verified. Simple structure makes the proposed antenna attractive for a wide range of applications in DOA estimation.

## ACKNOWLEDGMENT

The authors would like to thank Dr. Takayuki Tanaka, Saga University for his fruitful discussions. This work was supported in part by JSPS KAKENHI Grant Number 26420361 and 17K06429.

## REFERENCES

1. Merrill, I. S., *RADAR Handbook*, McGraw-Hill, 1990.
2. Mahafza, B. R., *Radar Systems Analysis and Design Using MATLAB*, Chapman & Hall/CRC, 2000.
3. Wang, H. and D. G. Fang, "A compact single layer monopulse microstrip antenna array," *IEEE Trans. Antennas and Propag.*, Vol. 54, No. 2, 503–509, 2006.

4. Zhong, W. U., G. M. Wang, and C. X. Zhang, "A broadband planar monopulse antenna array of C band," *IEEE Antenna and Wireless Propag. Letters*, Vol. 8, 1325–1328, 2009.
5. Hemant, K. and G. Kumar, "Microstrip antenna array with ratrace comparator at X-band for monopulse tracking radar," *2016 IEEE Int'l Symp. on Antennas and Propag. (APS-URSI)*, 513–514, Fajardo, Puerto Rico, 2016.
6. Fei, Y., Y. Xie, and L. Zhang, "Single patch antenna with monopulse patterns," *IEEE Microwave and Wireless Comp. Letters*, Vol. 26, 762–764, 2016.
7. Kederer, W. and J. Detlefsen, "Directon of Arrival (DOA) determination based on monopulse concepts," *Proc. 2000 Asia-Pacific Microwave Conf. (APMC2000)*, 120–123, Sydney, Australia, 2000.
8. Sakai, H., E. Nishiyama, and I. Toyoda, "Direction of arrival estimating array antenna," *Proc. 2012 Int'l Symp. on Antennas and Propag. (ISAP2012)*, POS 2-24, Nagoya, Japan, 2012.
9. Tanaka, R., E. Nishiyama, and I. Toyoda, "A mono-pulse DOA estimation antenna integrated with RF amplifiers and detection circuits," *2014 IEEE Int'l Symp. Antennas and Propag. and USNC-URSI Radio Sci. Mtg. (2014AP-S/USNC-URSI) Dig.*, 526.3, Memphis, USA, 2014.
10. Rashid, R., D. Hattori, E. Nisiyama, and I. Toyoda, "An RF multiplier integrated planar antenna for DOA estimation," *Proc. 2016 Int'l Symp. on Antennas and Propag. (ISAP2016)*, POS 1-77, 438–439, Okinawa, Japan, 2016.
11. Aikawa, M. and H. Ogawa, "Double-sided MICs and their applications," *IEEE Trans. Microwave Theory & Tech.*, Vol. 37, No. 2, 406–413, 1989.
12. Aikawa, M. and E. Nishiyama, "Compact MIC magic-T and the integration with planar array antenna," *IEICE Trans. Electron.*, Vol. E95-C, No. 10, 1560–1565, 2012.
13. Aikawa, M. and H. Ogawa, "A new MIC magic-T using coupled slotlines," *IEEE Trans. Microwave Theory & Tech.*, Vol. 28, No. 6, 523–528, 1980.
14. Hossain, M. A., Y. Ushijima, E. Nishiyama, I. Toyoda, and M. Aikawa, "Orthogonal circular polarization detection patch array antenna using double balanced RF multiplier," *Progress In Electromagnetics Research C*, Vol. 30, 65–80, 2012.